

**Strong Variation Of Electronic Properties Of MoS2 And WS2 Nanotubes
In Presence Of External Electric Fields**

Zibouche, N.; Philipsen, P.; Kuc, A.;

Originally published:

January 2019

Journal of Physical Chemistry C 123(2019)6, 3892-3899

DOI: <https://doi.org/10.1021/acs.jpcc.8b11411>

Perma-Link to Publication Repository of HZDR:

<https://www.hzdr.de/publications/Publ-28248>

Release of the secondary publication
on the basis of the German Copyright Law § 38 Section 4.

This document is confidential and is proprietary to the American Chemical Society and its authors. Do not copy or disclose without written permission. If you have received this item in error, notify the sender and delete all copies.

Strong Variation of Electronic Properties Of MoS₂ And WS₂ Nanotubes in Presence of External Electric Fields

Journal:	<i>The Journal of Physical Chemistry</i>
Manuscript ID	jp-2018-114119
Manuscript Type:	Article
Date Submitted by the Author:	26-Nov-2018
Complete List of Authors:	Zibouche, Nourdine; University of Oxford, Materials; University of Bath, Chemistry Philipsen, Pier; Software for Chemistry & Materials BV Kuc, Agnieszka; Helmholtz-Zentrum Dresden-Rossendorf,

SCHOLARONE™
Manuscripts

Strong Variation Of Electronic Properties Of MoS₂ And WS₂ Nanotubes In Presence Of External Electric fields

Nourdine Zibouche,^{*,†,‡} Pier Philipsen,[¶] and Agnieszka Kuc^{*,§}

[†]*Department of Chemistry, University of Bath, Claverton Down, Bath BA2 7AY, United Kingdom*

[‡]*Department of Materials, University of Oxford, Parks Road, Oxford OX1 3PH, United Kingdom*

[¶]*Software for Chemistry & Materials BV, De Boelelaan 1083, 1081 HV Amsterdam, The Netherlands*

[§]*Helmholtz-Zentrum Dresden-Rossendorf, Abteilung Ressourcenökologie, Forschungsstelle Leipzig, Permoserstr. 15, 04318 Leipzig, Germany*

E-mail: n.zibouche@bath.ac.uk; a.kuc@hzdr.de

Abstract

Transition-metal dichalcogenides (TMDCs) have recently attracted a huge international research focus from the point of two-dimensional (2D) materials. These materials also exist as nanotubes, however, they have been mostly studied for their lubricant properties. Despite their interesting electronic properties, that are quite similar to their 2D counterparts, these TMDC nanotubes remain much less explored. Like in 2D materials, the electronic properties of nanotubes can be strongly modulated by external means, such as strain or electric field. Here, we report on the effect of external electric fields on the electronic properties of MoS₂ and WS₂ nanotubes, using density functional theory. We show that the electric field induces a strong polarization in these nanotubes, what results in a nearly linear decrease of the band gaps with the field strength and eventually in a semiconductor-metal transition. In particular for large tube diameters, this transition can occur for field strengths between 1–2 V·nm⁻¹. This is an order of magnitude weaker than fields required to close the band gaps in the corresponding 2D mono- and bilayers of transition-metal dichalcogenides. We also observe splittings of the degenerate valence and conduction band states due to the Stark effect. Accordingly, such nanotubes could be used in nanoelectronics as logical switches, even at moderate field strengths that can be achieved experimentally, for example, by applying a gate voltage.

Keywords

Transition-metal dichalcogenides, nanotubes, electric field, ab initio calculations

Introduction

Molybdenum and tungsten disulfide (MoS₂ and WS₂) nanotubes (NTs) are one of the first synthesized and characterized tubular transition-metal dichalcogenides (TMDC)^{1,2} in the

1
2
3 early 1990's. TMDC-NTs can be thought of as cylindrical forms of their 2D layered counter-
4 parts. Similar to carbon, TMDC-NTs can be found in different chiralities, the most common
5 being zigzag and armchair, however, chiralities in between also exist. Such NTs are generally
6 synthesized as multi-wall (MW) nanotubes, but theoretical investigations of their properties
7 are most commonly performed on single-wall (SW) NT models. Depending on the chiral-
8 ity, SW TMDC-NTs are semiconductors with direct and indirect band gaps for zigzag and
9 armchair NTs, respectively.^{3,4} The band gap size of TMDC-NTs ranges between those of the
10 bulk and monolayered forms, increasing with the tube diameter.^{3,4}

11
12 For more than two decades, these inorganic nanotubes have mainly been investigated
13 for their tribological^{5,6} and mechanical properties.⁶⁻¹⁴ It has been shown that WS₂-NTs are
14 resistant to shock waves⁷ and exhibit ultrahigh strength and elasticity under uniaxial tensile
15 strain, with nearly linear strain-stress relation, up to the rupture point at about 10% strain.¹⁰
16 We have recently shown that tensile strain modulates the electronic and transport properties
17 of TMDC-NTs in a similar way as in the case of the corresponding 2D materials.¹³ However,
18 the transition from semiconducting to metallic character can be achieved only at very large
19 strain values, close to the rupture of the material.^{13,14} We have also shown that Raman
20 spectroscopy is suitable for monitoring the strain of individual tubes in the MW NTs.¹³
21 Other applications of TMDC-NTs have also been suggested, for example, as scanning probe
22 tips,¹⁵ catalysts,¹⁶ reinforcements for composite materials,¹⁷ photo-transistors,¹⁸ storage or
23 host materials.^{19,20}

24
25 Albeit the interesting properties of TMDC-NTs, studies of their applications in the field
26 of electronics remain insufficient in contrast to their layered 2D counterparts, which have
27 been intensively explored in the recent years.²¹⁻²⁷ Of particular interest, the effect of ex-
28 ternal electric field yield significant modifications on the electronic and optical properties
29 of 2D TMDCs.²⁸⁻³⁰ Similar findings are also shown for some nanotubular materials, includ-
30 ing carbon NTs,³¹⁻⁴² boron-nitride NTs,^{43,44} and zinc-oxide NTs.⁴⁵ However, the effect of
31 the applied electric field on the properties of TMDC-NTs is still a subject to be addressed.

1
2
3 We believe that only Wang and coworkers⁴⁶ examined the influence of a transverse electric
4 field on the structural and electronic properties of MoS₂ NTs. They showed that the band
5 gap of the MoS₂ linearly decreases with the increase of the electric field strength, resulting
6 in the semiconductor-metal transition for specific field magnitudes. Moreover, they found
7 that the effective masses of the charge carriers could be modulated by varying the electric
8 field strengths.⁴⁶ Therefore, it is intriguing to further investigate the peculiar properties of
9 these TMDC-NTs, particularly, for the control and the induced changes in their electronic
10 properties by means external fields.

11
12 In this work, we examine the response of zigzag and armchair MoS₂ and WS₂ NTs to the
13 external perpendicular electric field using density functional theory. We show that the band
14 gaps of these materials drastically reduce, even for weak electric fields, and the transition
15 from semiconductor to metal is rapidly attained for larger-diameter NTs. In the armchair
16 NTs, the polarization is found to be higher than the zigzag NTs and it increases with tube
17 diameter, which explains the quicker band-gap closure for these tubes. We also observe the
18 splitting of the degenerate band states close to the Fermi level due to the Stark effect in both
19 zigzag and armchair NTs. These properties suggest TMD-NTs as promising materials in the
20 applications of switchable nanoelectronics, even better than their 2D layered counterparts.

39 Methods

40
41 We have investigated single-walled MoS₂ and WS₂ nanotubes with the (n,0) zigzag and (n,n)
42 armchair chiralities for three selected diameter sizes (n = 18, 21, and 24) under external elec-
43 tric field, perpendicular to the tube axis (see Figure 1). All structures were fully optimized
44 (atomic positions and lattice vectors) using density functional theory as implemented in the
45 ADF-BAND software.^{47,48} The maximum gradient threshold for geometry optimization was
46 set to 10⁻³ hartree Å⁻¹.

47
48 The PBE⁴⁹ exchange-correlation functional was used together with the valence triple-

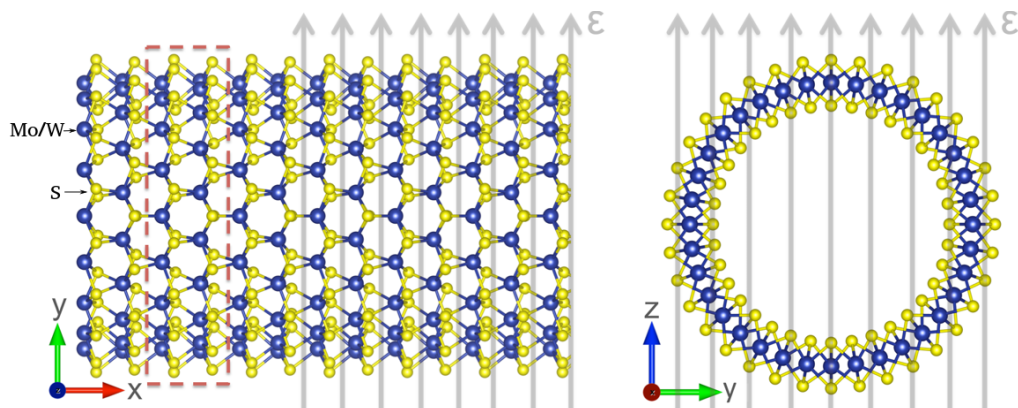


Figure 1: Atomic structure of TS_2 nanotubes (T - Mo, W;) in the perpendicular external electric field (ε). Side and top views are shown together with the lattice vectors and the unit cell (dashed rectangle). The transition-metal atoms are shown in blue and the sulfide atoms in yellow. This is an example of a zigzag type NT.

zeta polarized (TZP) basis sets composed of Slater-type and numerical orbitals with a small frozen core. Relativistic effects were taken into account by employing the scalar Zero Order Regular Approximation (ZORA).⁵⁰ The k-space integration was done with the 1D variant of the quadratic Wiesenekker-Baerends scheme,⁵¹ its k-space integration being set to 5, to ensure the convergence of the results.

A perturbation by means of a homogeneous external electric field was applied perpendicularly to the tube axis (of the relaxed geometries). The electric field strength was varied in the range of $0.0\text{--}4.0 \text{ V nm}^{-1}$. It is important to mention that we have not observed any geometry changes, when optimizing the systems in the presence of the electric field, for the field strengths employed in this work. On the other hand, it has been shown by Wang et al.⁴⁶ that for larger field strengths the geometry may be altered, resulting in an oval rather than circular geometries (in the cross-section of the tubes). In our work, we have applied fields much weaker than Wang et al.⁴⁶ to keep the geometries fairly unchanged.

Due to very large unit cells and, therefore, very expensive simulations, we have not taken into account the spin-orbit coupling in the electronic structure simulations. Therefore, the employed approach shows purely the electric-field-induced Stark effect in the band structures of TMDC-NTs.

Results Discussion

We have calculated the influence of the external perpendicular electric field on the band gap size and character in TMDC-NTs. Figure 2 shows the band gap evolution in (n,0) and (n,n) MoS₂ and WS₂ NTs as function of the field strength. All studied TMDC-NTs are semiconductors with band gaps (Δ) ranging from about 1 eV for (18,0) MoS₂ NT to about 2 eV for (24,24) WS₂ NT. This is in a good agreement with previous theoretical calculations.^{3,4} The band gap is, however, easily modulated by the electric field: we observe that Δ scales nearly linearly with the applied field, for the field strengths used in the present simulations. The (n,n) armchair NTs are more sensitive to the electric field and their band gaps close already for the field strength smaller than 2 V nm⁻¹, even though at the equilibrium, in the absence of the field, they have the largest Δ s. The corresponding zigzag NTs require about 1 V nm⁻¹ higher fields (about twice as the armchair NTs) to undergo the transition from semiconductors to metals. Moreover, the larger the diameter, the faster the band gap closure for both zigzag and armchair NTs.

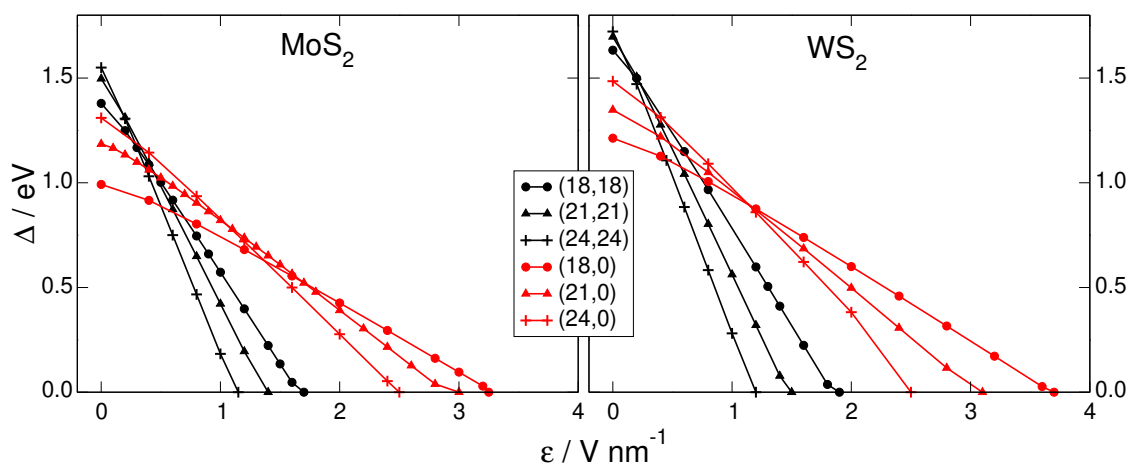


Figure 2: Band gap (Δ) evolution in the (n,0) and (n,n) MoS₂ and WS₂ NTs as function of the external perpendicular electric field (ε).

It is important to mention that the transition to the metallic state in TMDC-NTs occurs at the field values one order of magnitude smaller than for the corresponding 2D monolayers⁵² and 4-10 times smaller than for the bilayers.³⁰ We can conclude that NTs are more promising

building blocks for applications in switchable nanoelectronics than the corresponding layered systems.

In this study, we have focused on the single-walled NTs, however, inorganic NTs are often synthesized as multi-walled NTs. The electronic properties of these materials are expected to change even more drastically under the external electric field, similar to the corresponding multi-layered 2D TMDCs. Others and us have recently reported that TMDC bilayers undergo the semiconductor-metal transition for field strengths of 12–15 V nm⁻¹, 3–5 times (depending on the stoichiometry) significantly smaller than required for the monolayers.^{28–30} Moreover our unpublished research showed that for more layers (3–5 layers), this critical field further reduced with the number of layers.

The investigated NTs have large diameters, therefore, it is important to represent the change of the band gap as a drop of the potential (see Figure 3). The drop of the potential (U) is calculated as the electric field strength divided by the tube diameter, a value, which can be directly accessed experimentally. Our results show that potentials of 5.5–8.5 V and 6.0–9.5 V are needed to close the band gaps of MoS₂ and WS₂ NTs, respectively. Similar to the trends shown in Figure 2, armchair nanotubes with larger diameters are more sensitive and require less potential than zigzag nanotubes to undergo the transition to the metallic character.

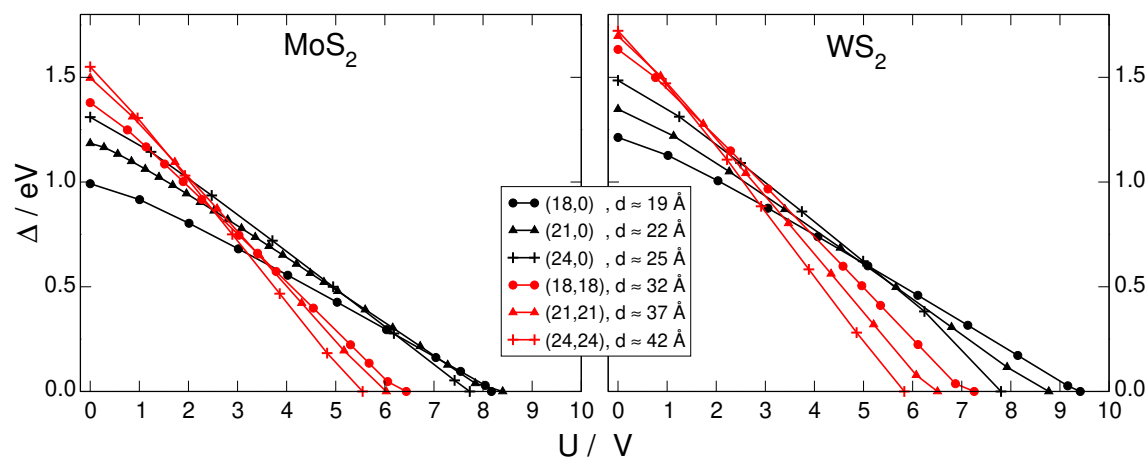


Figure 3: Band gap (Δ) evolution in the (n,0) and (n,n) MoS₂ and WS₂ nanotubes as function of the drop of the potential (U).

The applied perpendicular electric fields induce dipole moments perpendicular to the tube axis (see Figure 4). These induced dipole moments (μ) increase linearly with the field strength, similar to the 2D materials,^{30,52} however, in the case of NTs, the values are an order of magnitude larger. The polarization of the NTs is higher for armchair systems and increases with the tube diameter, what explains the quicker band-gap closure for these tubes. These results are expected, because the charge separation increases with the tube diameter, resulting in increased μ . Therefore, we can conclude that the band gaps of large-diameter TMDC-NTs can be tuned more easily using already weak electric fields.

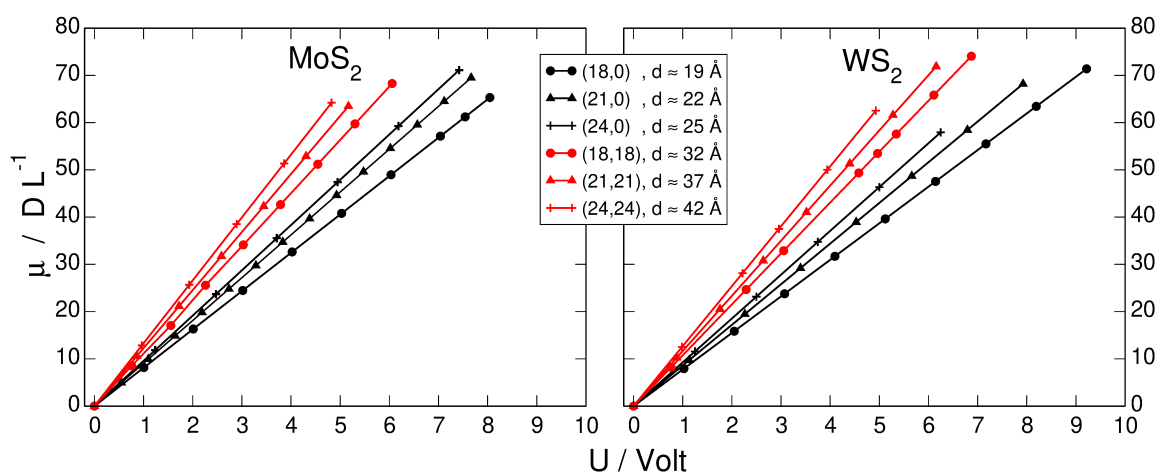


Figure 4: Dipole moments (μ) in the (n,0) and (n,n) MoS₂ and WS₂ nanotubes as function of the external electric field (ε).

The band structures of TMDC-NTs in the presence of external electric fields are shown in Figure 5 for the largest tube-diameters studied in this work, as examples. As discussed in earlier works,^{3,4} the general trend in the absence of the electric field is that the zigzag and armchair NTs are direct and indirect band-gap semiconductors, respectively. Before any electric field is applied, the tubes are perfectly symmetric and, therefore, without spin-orbit coupling, the valence band maximum (VBM) and the conduction band minimum (CBM) are degenerate and no band splitting is observed. VBM and CBM of the zigzag NTs are situated at the Γ point, whereas for the armchair NTs they are situated at the Γ and K points (point at 2/3 between Γ and X), respectively. Figure S1 shows the change in the

band edge positions with respect to the applied electric field. The field shifts the VBM to higher energies, while CBM lowers in energy, eventually converging to the same values for both band edges at the critical field strengths, the point of the transition to the metallic systems.

Under external electric field, the band gap character (direct or indirect) does not change until the critical point. Moreover, the field induces splitting in both VBM and CBM of armchair NTs. Since we have not taken into account any spin-orbit coupling in the present study, the splitting is purely due to the so-called Stark effect, as a result of the applied electric field. The splitting values (Δ_{split}) are proportional to the field strength and the maximum values at the critical points are shown in Table S1. The values of Δ_{split} at Γ and K generally decrease with the tube diameter. Similar trend is observed for the valence band of zigzag NTs, with the VBM at Γ point.

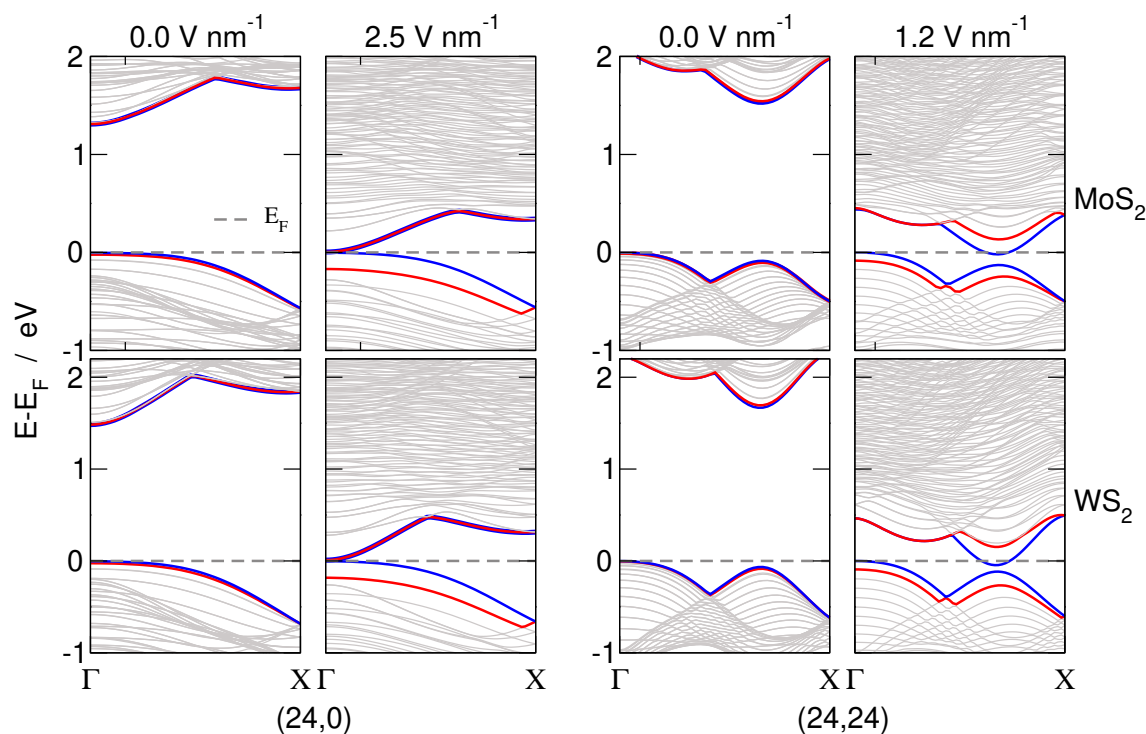


Figure 5: Band structures of (24,0) and (24,24) MoS₂ and WS₂ nanotubes at selected external electric fields: 0.0 V nm⁻¹ corresponding to no applied field, 2.5 and 1.2 V nm⁻¹ corresponding to the critical electric fields, when the band gaps close for the zigzag and armchair NTs, respectively.

The calculated effective masses of electrons (m_e^*) and holes (m_h^*) with respect to the electric field are shown in Figure 6. In general, m_e^* increase and m_h^* decrease with the field strength, meaning the electrons become heavier and holes become lighter. However, the absolute values of both carriers are different by one order of magnitude, ranging between 0.3 and 0.6 m_0 for electrons and between 3.0 and 11.0 m_0 for holes. The holes are so heavy, because the VBMs are flat and almost dispersionless in the vicinity of the Γ point. These values are much larger than the corresponding numbers found in the TMDC 2D layered systems. At the same time, owing to the strong dispersion in the conduction bands, the electrons are very light, smaller than the corresponding values in 2D materials, both mono- and bilayers.

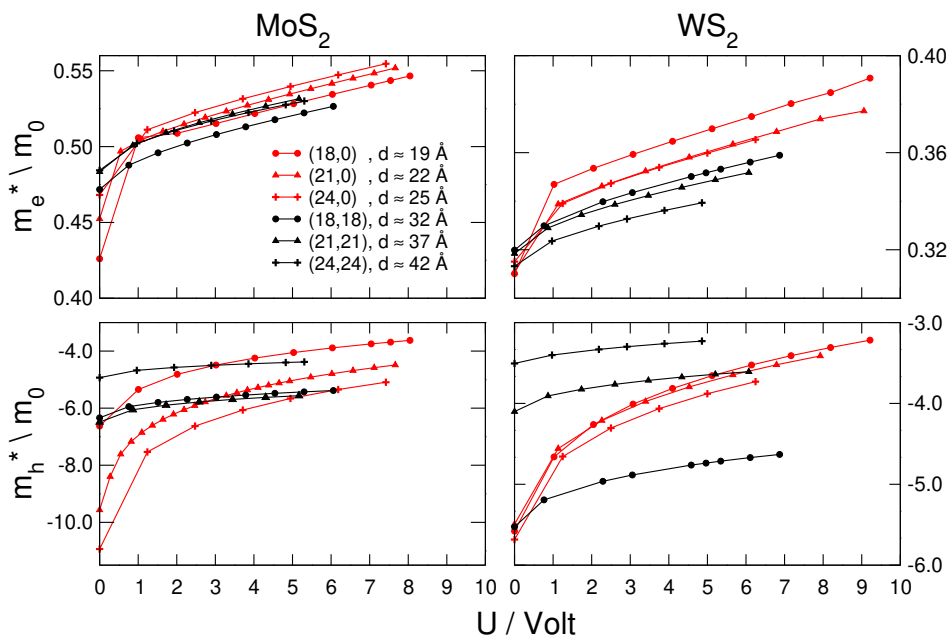


Figure 6: Electron and hole effective masses in (n,0) and (n,n) MoS₂ and WS₂ nanotubes as function of the external electric field.

At zero electric field, m_e^* of MoS₂ NTs are by at least 0.1 m_0 larger than those of WS₂ NTs. They change nearly linearly with the applied field for strengths above 0.5 V nm⁻¹. Because the TMDC-NTs have very heavy holes and very light electrons, they are promising materials for ultra-short field effect transistors, as this feature would prevent the intra-band tunneling.^{18,53,54}

Conclusions

We have studied the response of MoS₂ and WS₂ nanotubes to the external perpendicular electric field, by means of density functional theory. We have shown that the potential gradients cause a linear reduction of the band gaps and an increase of the induced dipole moments, what eventually results in a semiconductor-metal transition, at critical field strengths. The polarization is found to be stronger for armchair NTs and tubes with larger diameters. Compared to the corresponding 2D mono- and bilayer TMDCs, the critical fields necessary to close the band gaps are by one order of magnitude smaller for the tubular systems, making them more promising building blocks for applications in switchable nanoelectronics.

The band structure analysis shows that the indirect and direct band gap characters are preserved under the applied electric fields until the band gap closure. Moreover, the degeneracy of band edges is altered, a band splitting occurs, resulting in the so-called Stark effect. This effect results also in the changes of the charge-carrier mobilities. The effective masses of the electrons (holes) are in general small (large) for the range of field strengths used in the present work. This leads to a conclusion that TMDC-NTs are very valuable candidates for logical devices, especially at the ultra-short scale.

Notes

The authors declare no competing financial interest.

Acknowledgement

We thank Prof. Thomas Heine for his insightful comments and helpful discussions that greatly improved the manuscript. The authors acknowledge the University of Oxford Advanced Research Computing (ARC) facility (<http://dx.doi.org/10.5281/zenodo.22558>) and ZIH Dresden for providing computational resources.

References

- (1) Tenne, R.; Margulis, L.; Genut, M.; Hodes, G. Polyhedral And Cylindrical Structures Of Tungsten Disulfide. *Nature* **1992**, *360*, 444.
- (2) Margulis, L.; Salitra, G.; Tenne, R.; Talianker, M. Nested Fullerene-like Structures. *Nat* **1993**, *365*, 113–114.
- (3) Seifert, G.; Terrones, H.; Terrones, M.; Jungnickel, G.; Frauenheim, T. Structure and electronic properties of MoS₂ nanotubes. *Phys. Rev. Lett.* **2000**, *85*, 146.
- (4) Zibouche, N.; Kuc, A.; Heine, T. From layers to nanotubes: Transition metal disulfides TMS₂. *The European Physical Journal B* **2012**, *85*, 49.
- (5) Rapoport, L.; Bilik, Y.; Feldman, Y.; Homyonfer, M.; Cohen, S. R.; Tenne, R. Hollow nanoparticles of WS₂ as potential solid-state lubricants. *Nature* **1997**, *387*, 791–793.
- (6) Kaplan-Ashiri, I.; Cohen, S. R.; Gartsman, K.; Rosentsveig, R.; Ivanovskaya, V.; Heine, T.; Seifert, G.; Wagner, H. D.; Tenne, R. Direct tensile tests of individual WS₂ nanotubes. *Prism 5: The Fifth Pacific Rim International Conference On Advanced Materials And Processing, Pts 1-5* **2005**, *475-479*, 4097–4102.
- (7) Zhu, Y. Q.; Sekine, T.; Brigatti, K. S.; Firth, S.; Tenne, R.; Rosentsveig, R.; Kroto, H. W.; Walton, D. R. M. Shock-Wave Resistance of WS₂ Nanotubes. *Journal of the American Chemical Society* **2003**, *125*, 1329–1333.
- (8) Kaplan-Ashiri, I.; Cohen, S. R.; Gartsman, K.; Rosentsveig, R.; Ivanovskaya, V.; Heine, T.; Seifert, G.; Wagner, H. D.; Tenne, R. Mechanical properties of individual WS₂ nanotubes. *Electronic Properties Of Synthetic Nanostructures* **2004**, *723*, 306–312.
- (9) Kaplan-Ashiri, I.; Cohen, S. R.; Gartsman, K.; Rosentsveig, R.; Seifert, G.; Tenne, R.

- Mechanical behavior of individual WS₂ nanotubes. *Journal Of Materials Research* **2004**, *19*, 454–459.
- (10) Kaplan-Ashiri, I.; Cohen, S. R.; Gartsman, K.; Rosentsveig, R.; Ivanovskaya, V. V.; Heine, T.; Seifert, G.; Wagner, H. D.; Tenne, R. On the Mechanical Behavior of Tungsten Disulfide Nanotubes under Axial Tension and Compression. *Proceedings of the National Academy of Sciences of the USA* **2006**, *103*, 523.
- (11) Tang, D.-M.; Wei, X.; Wang, M.-S.; Kawamoto, N.; Bando, Y.; Zhi, C.; Mitome, M.; Zak, A.; Tenne, R.; Golberg, D. Revealing the Anomalous Tensile Properties of WS₂ Nanotubes by in Situ Transmission Electron Microscopy. *Nano Letters* **2013**, *13*, 1034–1040.
- (12) Kaplan-Ashiri, I.; Tenne, R. Mechanical Properties of WS₂ Nanotubes. *Journal of Cluster Science* **2007**, *18*, 549.
- (13) Ghorbani-Asl, M.; Zibouche, N.; Wahiduzzaman, M.; Oliveira, A. F.; Kuc, A.; Heine, T. Electromechanics in MoS₂ and WS₂: nanotubes vs. monolayers. *Scientific Reports* **2013**, *3*.
- (14) Zibouche, N.; Ghorbani-Asl, M.; Heine, T.; Kuc, A. Electromechanical Properties of Small Transition-Metal Dichalcogenide Nanotubes. *Inorganics* **2014**, *2*, 155–167.
- (15) Rothschild, A.; Cohen, S. R.; Tenne, R. WS₂ nanotubes as tips in scanning probe microscopy. *Applied Physics Letters* **1999**, *75*, 4025–4027.
- (16) Komarneni, M. R.; Yu, Z.; Burghaus, U.; Tsverin, Y.; Zak, A.; Feldman, Y.; Tenne, R. Characterization of Ni-Coated WS₂ Nanotubes for Hydrodesulfurization Catalysis. *Israel Journal of Chemistry* **2012**, *52*, 1053–1062.
- (17) Zhang, W.; Ge, S.; Wang, Y.; Rafailovich, M.; Dhez, O.; Winesett, D.; Ade, H.; Shafi, K. V.; Ulman, A.; Popovitz-Biro, R. et al. Use of functionalized {WS₂} nan-

- 1
2
3
4
5
6
7
8
9
10
11
12
13
14
15
16
17
18
19
20
21
22
23
24
25
26
27
28
29
30
31
32
33
34
35
36
37
38
39
40
41
42
43
44
45
46
47
48
49
50
51
52
53
54
55
56
57
58
59
60
- otubes to produce new polystyrene/polymethylmethacrylate nanocomposites. *Polymer* **2003**, *44*, 2109 – 2115.
- (18) Unalan, H. E.; Yang, Y.; Zhang, Y.; Hiralal, P.; Kuo, D.; Dalal, S.; Butler, T.; Cha, S. N.; Jang, J. E.; Chremmou, K. et al. ZnO Nanowire and WS₂ Nanotube Electronics. *IEEE Transactions on Electron Devices* **2008**, *55*, 2988–3000.
- (19) Wang, G. X.; Bewlay, S.; Yao, J.; Liu, H. K.; Dou, S. X. Tungsten Disulfide Nanotubes for Lithium Storage. *Electrochem. Solid-State Lett* **2004**, *7*.
- (20) Hua, M.; Zhanliang, T.; Feng, G.; Jun, C.; Huatang, Y. Synthesis, characterization and hydrogen storage capacity of MS₂ (M = Mo, Ti) nanotubes. *Frontiers of Chemistry in China* **2006**, *1*, 260–263.
- (21) Jariwala, D.; Sangwan, V. K.; Lauhon, L. J.; Marks, T. J.; Hersam, M. C. Emerging Device Applications for Semiconducting Two-Dimensional Transition Metal Dichalcogenides. *ACS Nano* **2014**, *8*, 1102–1120.
- (22) Dubertret, B.; Heine, T.; Terrones, M. The Rise of Two-Dimensional Materials. *Accounts of Chemical Research* **2015**, *48*, 1–2.
- (23) Kuc, A.; Heine, T.; Kis, A. Electronic properties of transition-metal dichalcogenides. *MRS Bulletin* **2015**, *40*, 577–584.
- (24) Duan, X.; Wang, C.; Pan, A.; Yu, R.; Duan, X. Two-dimensional transition metal dichalcogenides as atomically thin semiconductors: opportunities and challenges. *Chem. Soc. Rev.* **2015**, *44*, 8859–8876.
- (25) Choi, W.; Choudhary, N.; Han, G. H.; Park, J.; Akinwande, D.; Lee, Y. H. Recent development of two-dimensional transition metal dichalcogenides and their applications. *Materials Today* **2017**, *20*, 116 – 130.

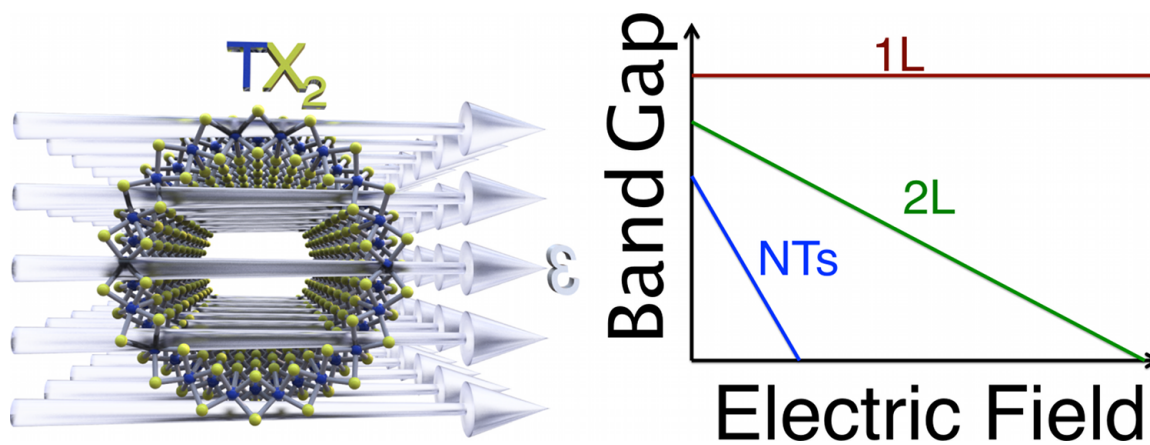
- 1
2
3 (26) Hu, Y.; Huang, Y.; Tan, C.; Zhang, X.; Lu, Q.; Sindoro, M.; Huang, X.; Huang, W.;
4 Wang, L.; Zhang, H. Two-dimensional transition metal dichalcogenide nanomaterials
5 for biosensing applications. *Mater. Chem. Front.* **2017**, *1*, 24–36.
6
7
8
9
10 (27) Li, H.; Li, Y.; Aljarb, A.; Shi, Y.; Li, L.-J. Epitaxial Growth of Two-Dimensional
11 Layered Transition-Metal Dichalcogenides: Growth Mechanism, Controllability, and
12 Scalability. *Chemical Reviews* **2018**, *118*, 6134–6150.
13
14
15
16 (28) Ramasubramaniam, A.; Naveh, D.; Towe, E. Tunable band gaps in bilayer transition-
17 metal dichalcogenides. *Phys. Rev. B* **2011**, *84*, 205325.
18
19
20
21 (29) Liu, Q.; Li, L.; Li, Y.; Gao, Z.; Chen, Z.; Lu, J. Tuning Electronic Structure of Bilayer
22 MoS₂ by Vertical Electric Field: A First-Principles Investigation. *J. Phys. Chem. C.*
23 **2012**, *116*, 21556–21562.
24
25
26
27
28 (30) Zibouche, N.; Philipsen, P.; Kuc, A.; Heine, T. Transition-metal dichalcogenide bilayers:
29 Switching materials for spintronic and valleytronic applications. *Phys. Rev. B* **2014**,
30 *90*, 125440.
31
32
33
34
35 (31) Kim, C.; Kim, B.; Lee, S. M.; Jo, C.; Lee, Y. H. Effect of electric field on the electronic
36 structures of carbon nanotubes. *Applied Physics Letters* **2001**, *79*, 1187–1189.
37
38
39
40 (32) Rochefort, A.; Di Ventura, M.; Avouris, P. Switching behavior of semiconducting carbon
41 nanotubes under an external electric field. *Applied Physics Letters* **2001**, *78*, 2521–2523.
42
43
44
45 (33) Li, Y.; Rotkin, S. V.; Ravaioli, U. *Electronic Response and Bandstructure Modulation*
46 *of Carbon Nanotubes in a Transverse Electrical Field*; 2003; Vol. 3; pp 183–187.
47
48
49
50 (34) Guo, W.; Guo, Y. Giant Axial Electrostrictive Deformation in Carbon Nanotubes.
51 *Phys. Rev. Lett.* **2003**, *91*, 115501.
52
53
54
55 (35) Li, Y.; Rotkin, S.; Ravaioli, U. Influence of external electric fields on electronic response
56
57
58
59
60

- 1
2
3 and bandstructure of carbon nanotubes. *Nanotechnology*, 2003. IEEE-NANO 2003.
4
5 2003 Third IEEE Conference on. 2003.
6
7
- 8 (36) Rocha, C. G.; Pacheco, M.; Barticevic, Z.; Latgè, A. Electric and magnetic field effects
9 on electronic structure of straight and toroidal carbon nanotubes. *Brazilian Journal of*
10
11 *Physics* **2004**, *34*, 644 – 646.
12
13
- 14 (37) Tien, L.-G.; Tsai, C.-H.; Li, F.-Y.; Lee, M.-H. Band-gap modification of defective carbon
15 nanotubes under a transverse electric field. *Phys. Rev. B* **2005**, *72*, 245417.
16
17
- 18 (38) Shtogun, Y. V.; Woods, L. M. Electronic Structure Modulations of Radially Deformed
19 Single Wall Carbon Nanotubes under Transverse External Electric Fields. *The Journal*
20
21 *of Physical Chemistry C* **2009**, *113*, 4792–4796.
22
23
- 24 (39) Yamanaka, A.; Okada, S.; Kim, G.; Bernholc, J.; Kwon, Y.-K. Electronic Properties of
25 Carbon Nanotubes under an Electric Field. *Applied Physics Express* **2012**, *5*, 095101.
26
27
- 28 (40) Yamanaka, A.; Okada, S. Electronic Properties of Carbon Nanotubes under an Electric
29 Field. *Applied Physics Express* **2012**, *5*, 095101.
30
31
- 32 (41) Yamanaka, A.; Okada, S. Electronic Properties of Capped Carbon Nanotubes under an
33 Electric Field: Inhomogeneous Electric-Field Screening Induced by Bond Alternation.
34
35 *Japanese Journal of Applied Physics* **2013**, *52*, 06GD04.
36
37
- 38 (42) Yamanaka, A.; Okada, S. Anomalous Electric-Field Screening at the Edge Atomic Sites
39 of Finite-Length Zigzag Carbon Nanotubes. *Applied Physics Express* **2013**, *6*, 045101.
40
41
- 42 (43) Khoo, K. H.; Mazzoni, M. S. C.; Louie, S. G. Tuning the electronic properties of boron
43 nitride nanotubes with transverse electric fields: A giant dc Stark effect. *Phys. Rev. B*
44
45 **2004**, *69*, 201401.
46
47
- 48 (44) Freitas, A.; Azevedo, S.; Kaschny, J.; Machado, M. Electric field effect on the electronic
49
50
51
52
53
54
55
56
57
58
59
60

- 1
2
3 properties of double-walled carbon-doped boron-nitride nanotubes. *Applied Physics A*
4 **2014**, *114*, 1039–1048.
5
6
7
- 8 (45) Wang, Y.; Wang, B.; Zhang, Q.; Zhao, J.; Shi, D.; Yunoki, S.; Kong, F.; Xu, N.
9 Tunable deformation and electronic properties of single-walled ZnO nanotubes under a
10 transverse electric field. *Journal of Applied Physics* **2012**, *111*, 073704.
11
12
13
- 14 (46) Wang, Y.; Chen, Y. Study on Waterfront Landscape Design Based on Regional Culture.
15 Hydraulic Engineering and Sustainable City Development III. 2014; pp 493–496.
16
17
18
- 19 (47) te Velde, G.; Baerends, E. J. Precise density-functional method for periodic structures.
20 *Phys. Rev. B* **1991**, *44*, 7888–7903.
21
22
23
- 24 (48) Philipsen, P. H. T.; te Velde, G.; Baerends, E. J.; Berger, J.; de Boeij, P. L.; Groen-
25 veld, J.; Kadantsev, E. S.; Klooster, R.; Kootstra, F.; Romaniello, P. et al. BAND2012,
26 SCM, Theoretical Chemistry, Vrije Universiteit, Amsterdam, Netherlands. 2012.
27
28
29
- 30 (49) Perdew, J. P.; Burke, K.; Ernzerhof, M. Generalized gradient approximation made
31 simple. *Phys. Rev. Lett.* **1996**, *77*, 3865.
32
33
34
- 35 (50) Philipsen, P. H. T.; van Lenthe, E.; Snijders, J. G.; Baerends, E. J. Relativistic cal-
36 culations on the adsorption of CO on the (111) surfaces of Ni, Pd, and Pt within the
37 zeroth-order regular approximation. *Phys. Rev. B* **1997**, *56*, 13556–13562.
38
39
40
- 41 (51) Wiesenekker, G.; Baerends, E. J. Quadratic and cubic tetrahedron methods for Brillouin
42 zone integration. *Computer Physics Communications* **2005**, *167*, 85.
43
44
45
- 46 (52) Zibouche, N.; Philipsen, P.; Heine, T.; Kuc, A. Electron transport in MoWSeS mono-
47 layers in the presence of an external electric field. *Phys. Chem. Chem. Phys.* **2014**, *16*,
48 11251–11255.
49
50
51
- 52 (53) Levi, R.; Bitton, O.; Leitus, G.; Tenne, R.; Joselevich, E. Field-Effect Transistors
53
54
55
56
57
58
59
60

1
2
3 Based on WS₂ Nanotubes with High Current-Carrying Capacity. *Nano Letters* **2013**,
4 *13*, 3736–3741.
5
6

7
8 (54) Strojnik, M.; Kovic, A.; Mrzel, A.; Buh, J.; Strle, J.; Mihailovic, D. MoS₂ nanotube
9 field effect transistors. *AIP Advances* **2014**, *4*, 097114.
10
11



26
27
28
29
30
31
32
33
34
35
36
37
38
39
40
41
42
43
44
45
46
47
48
49
50
51
52
53
54
55
56
57
58
59
60

Figure 7: TOC figure